

Supplementary Materials

Chlorine Functionalized Keto-Enamine Based Covalent Organic Frameworks for CO₂ Separation and Capture

*Digambar B. Shinde^{1,§}, Mayur Ostwal^{1,§}, Xinbo Wang¹, Amol M. Hengne², Yang Liu¹, Guan Sheng¹, Kuo-Wei Huang², and Zhiping Lai**

¹Advanced Membranes and Porous Materials Center, Division of Physical Science and Engineering, King Abdullah University of Science and Technology (KAUST), Thuwal, Saudi Arabia

²Catalysis Center, Division of Physical Science and Engineering, King Abdullah University of Science and Technology (KAUST), Thuwal, Saudi Arabia

[§]These authors contributed equally for this work

* Corresponding author E-mail: Zhiping.lai@kaust.edu.sa

1. Materials and Characterization tools:

1.1 Materials:

Anhydrous 1,4-dioxane, mesitylene (98%), phloroglucinol, hexamethylenetetramine, trifluoroacetic acid, anhydrous sodium sulfate, 2,5-dichloro-1,4-phenylene diamine, 3,3'-dichlorobenzidine, glacial acetic acid and acetone were all purchased from Sigma-Aldrich and used without further purification.

1.2 Characterization tools:

Fourier transform infrared (FT-IR): The FTIR measurements was carried out on Nicolet iS10 FTIR spectrometer ranging from 4000 to 525 cm⁻¹.

Powder X-ray diffraction (PXRD): PXRD measurement were carried out on Bruker D8-advance diffractometer in reflectance Bragg-Brentano geometry employing Ni filtered Cu K α line focused radiation at 1600 W (40 kV, 40 mA) power and equipped with a Na(Tl) scintillation detector fitted at 0.3 mm radiation entrance slit.

Scanning electron microscopy (SEM): The SEM images were taken on Magellan XHR SEM.

1.3 Synthesis of CAA-COF-1 and CAA-COF-2 by the solvothermal method:

The synthesis of COFs (**CAA-COF-1** and **CAA-COF-2**) in pyrex glass tube (o.d. \times i.d. = 22 \times 12 mm² and length 18 cm) the starting material is 1,3,5-triformylphloroglucinol (TFA) (63.0 mg, 0.30 mmol) and 2,5-Dichloro-1,4-phenylene diamine (2,5-DCA) (79.6 mg, 0.45 mmol) or 3,3'-Dichlorobenzidine (3,3'-DCB) (146.6 mg, 0.45 mmol) and 4.5 mL of mesitylene and 1.0 mL of 1,4-dioxane, 0.4 mL of 6.0 M aqueous acetic acid. The resulting mixture was sonicated for 10-15 minutes for homogenous dispersion. The glass tube was then flash frozen at 77 K in liquid N₂ bath and then degassed by the freeze-pump-thaw cycle for 2 to 3 times to ensure the removal of dissolved gases. The tube was sealed off and then heated at 120 °C for 72h. A dark red colored precipitate formed was filtered through the whatmann filtre paper and washed with 5-6 times with mesitylene, water and then acetone. The powder collected was then solvent exchanged with acetone three times and then dried at 150 °C under vacuum for 24 hours to give a dark red colored powder in 86 % isolated yield. The elemental micro analysis (C, N, H and Cl) of the COFs and the experimental data are very well matched to the theoretical. This is indicating the purity of the material.

CAA-COF-1:

IR (powder): ν_{\max} 1575, 1442, 1246, 1068, 1046, 1022 and 845 cm⁻¹;

¹³CSSNMR: 107.7, 116.2, 124.2, 132.5, 146.3 and 184.1;

Elemental Analysis data: Anal. Calcd. For C₆ClONH₃: C, 51.28; H, 2.15; N, 9.97; Cl, 25.22
found: C, 52.47; H, 2.89; N, 10.09; Cl, 25.76.

CAA-COF-2:

IR (powder): ν_{\max} 1582, 1441, 1262, 1047, 1025, 1011 and 826 cm⁻¹;

¹³CSSNMR: 108.1, 115.3, 124.1, 132.7, 146.1 and 184.3;

Elemental Analysis data: Anal. Calcd. For C₉ClONH₃: C, 60.87; H, 2.27; N, 7.89; Cl, 19.96
found: C, 61.29; H, 3.01; N, 8.14; Cl, 20.57.

2. COFs characterization:

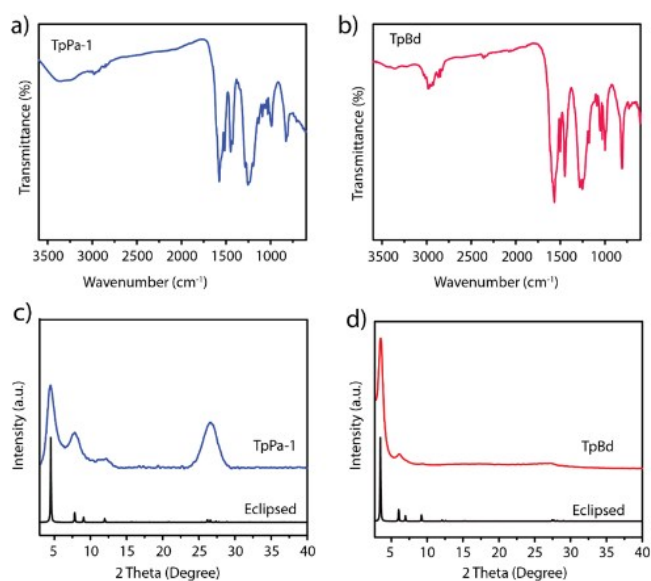


Figure S1: (a) FT-IR spectra of TpPa-1; (b) FT-IR spectra of TpBd; (c) PXRD data of TpPa-1 and compared with eclipsed structure; (d) PXRD data of TpBd and compared with eclipsed structure

Table S1. Fractional atomic coordinates for the unit cell of CAA-COF-1

CAA-COF-1			
<i>P6/m space group, $a = b = 22.55$, $c = 3.4 \text{ \AA}$; $\alpha = \beta = 90.0$, $\gamma = 120.0$</i>			
O1	0.28355	0.52709	0.5
N1	0.41129	0.55212	0.5
C1	0.30695	0.59146	0.5
C2	0.38113	0.64063	0.5
C3	0.42797	0.61784	0.5
C4	0.45481	0.52704	0.5
C5	0.42936	0.4559	0.5
C6	0.52674	0.57065	0.5
C11	0.34128	0.40231	0.5

Table S2. Fractional atomic coordinates for the unit cell of CAA-COF-2

CAA-COF-2			
<i>P6/m space group, a = b = 30.48, c = 3.39 Å, α = β = 90.0, γ = 120.0</i>			
O1	0.2956	0.5612	0
N2	0.3872	0.5781	0
C1	0.3135	0.6107	0
C2	0.4039	0.6298	0
C3	0.4195	0.5569	0
C4	0.4739	0.5883	0
C5	0.5046	0.5656	0
C6	0.4829	0.5112	0
C7	0.4281	0.4803	0
C8	0.3968	0.5027	0
C9	0.3684	0.6472	0
Cl1	0.33219	0.46441	0

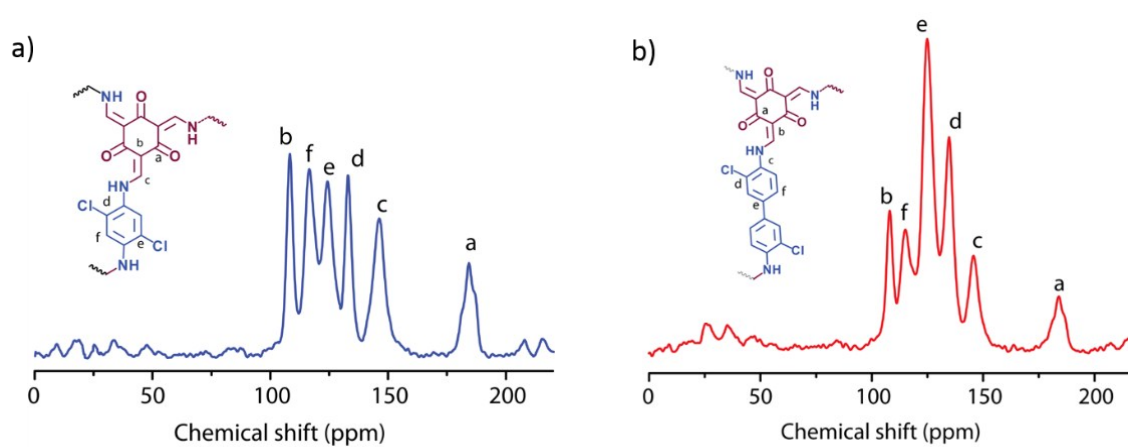


Figure S2: (a) ¹³C CP-MAS spectrum of CAA-COF-1 and (b) CAA-COF-2.

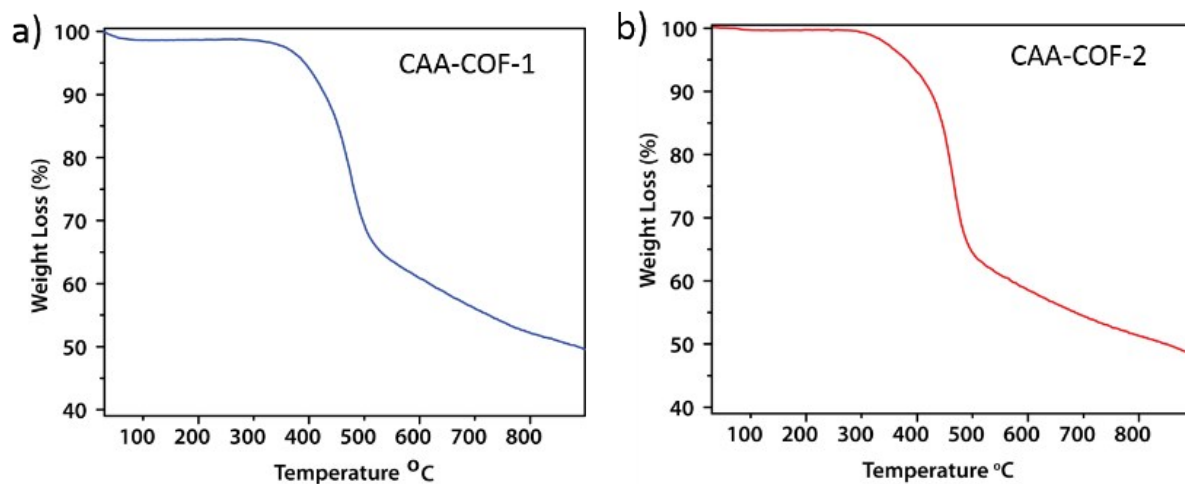


Figure S3: (a) TGA data of CAA-COF-1 and (b) CAA-COF-2 under N₂ atmosphere.

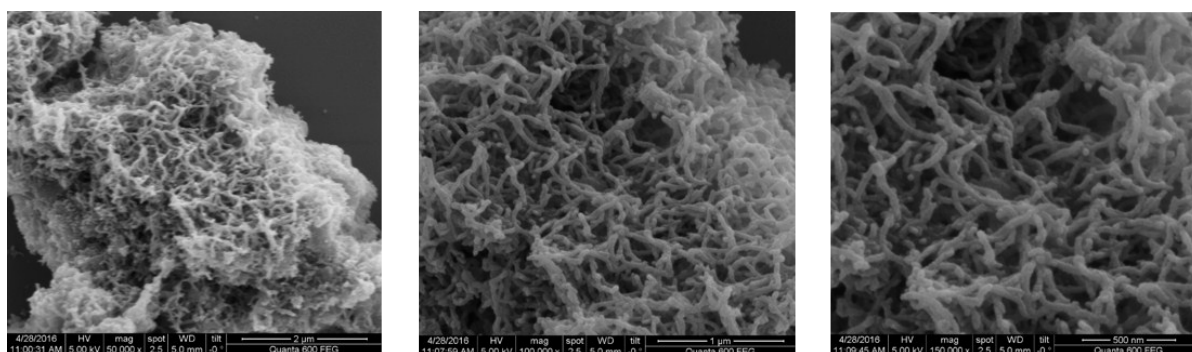


Figure S4: SEM images of CAA-COF-1.

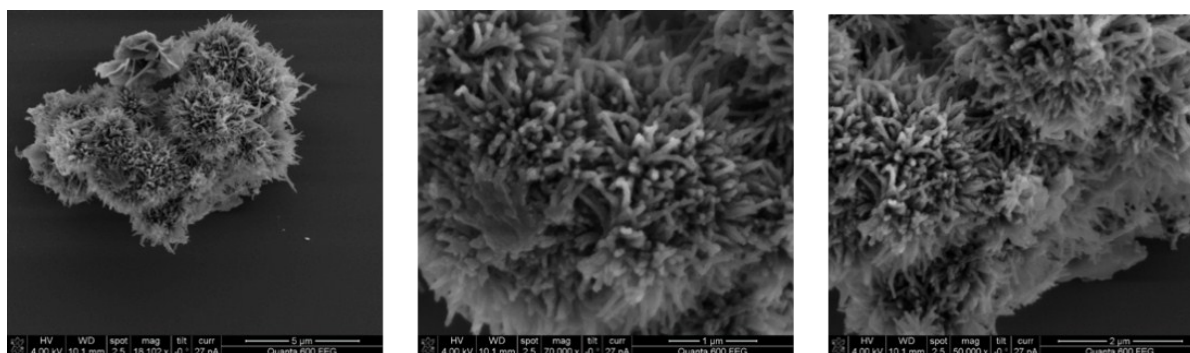


Figure S5: SEM images of CAA-COF-2.

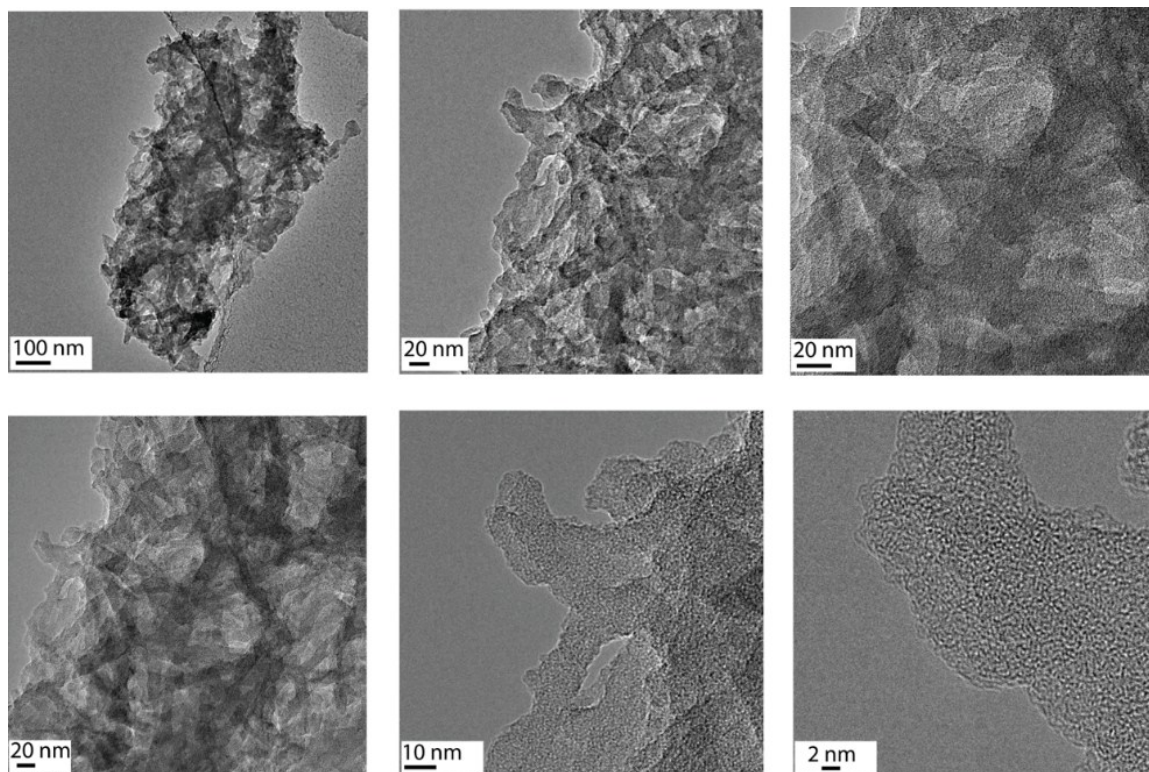


Figure S6: TEM images of CAA-COF-1.

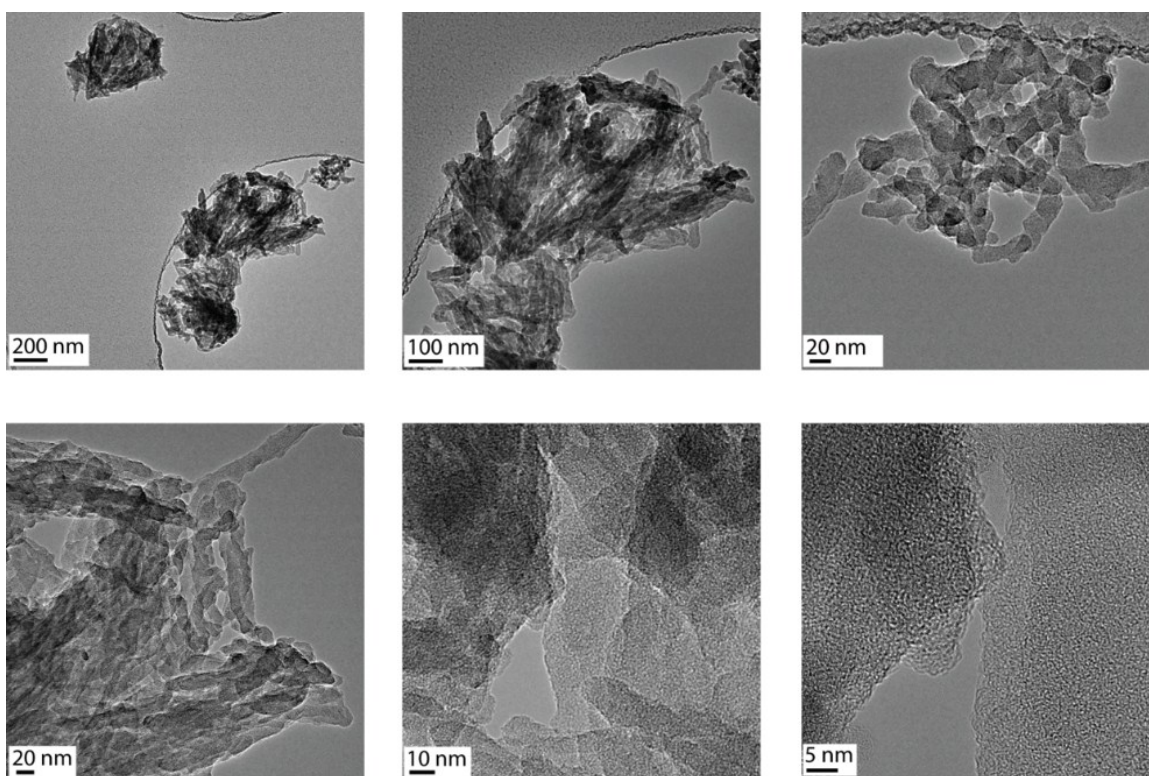


Figure S7: TEM images of CAA-COF-2.

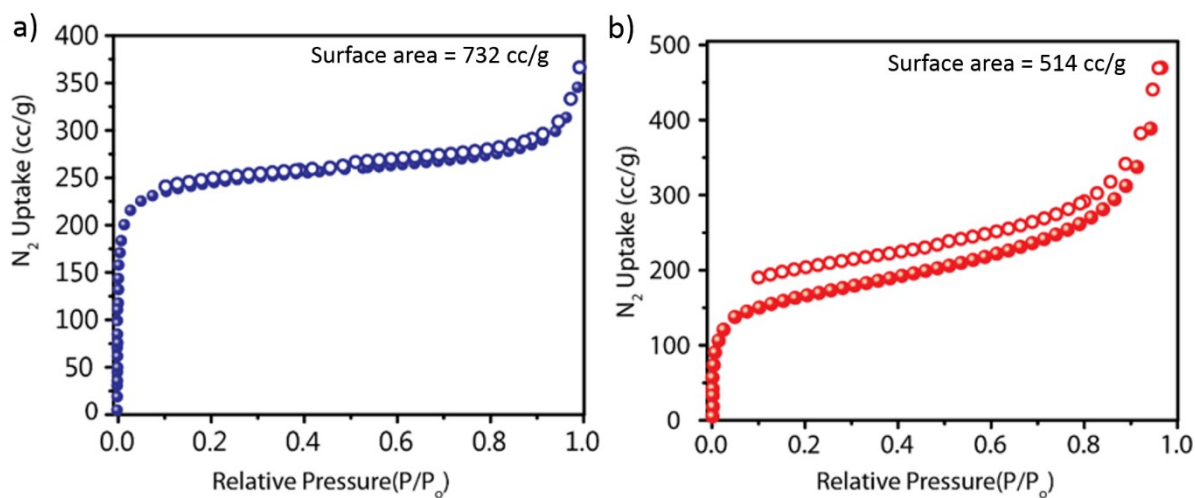


Figure S8: (a) N_2 adsorption isotherm of TpPa-1 and (b) N_2 adsorption isotherm of TpBd at 77K.

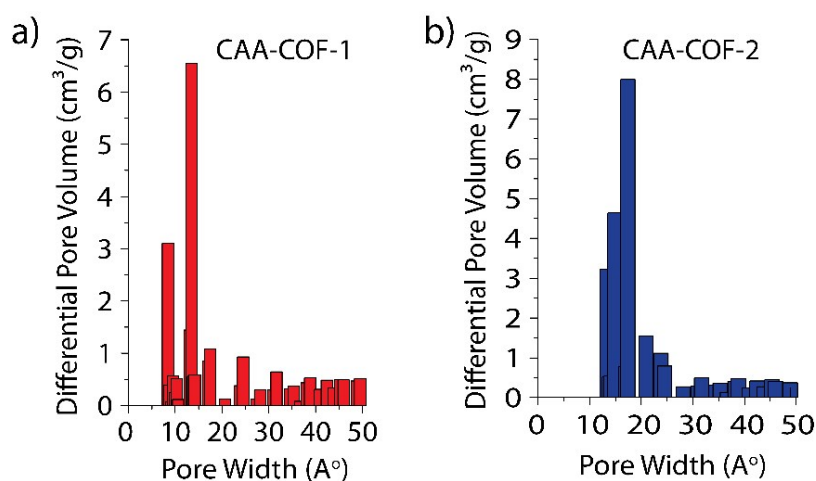


Figure S9: (a) Pore size distribution of CAA-COF-1 and (b) CAA-COF2 by NLDFT method from N_2 adsorption data

(After treatment with acid or base, the relative intensity decreases (without change in peak position, thus very limited loss of crystallinity (d-spacing) and we believe this may be due to loss of long range order in materials after the harsh chemical treatment.)

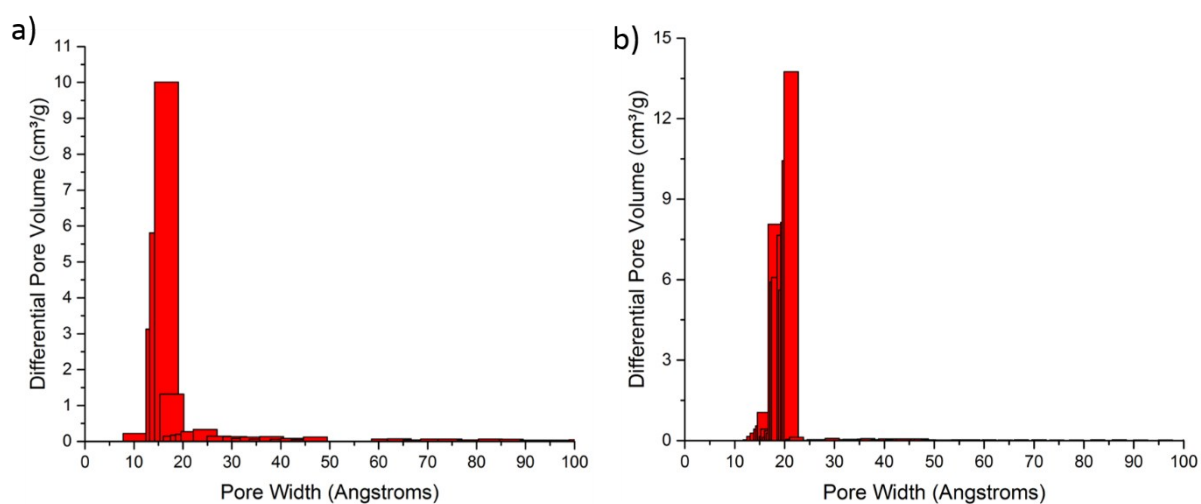


Figure S10: (a) Pore size distribution of TpPa-1 and (b) TpBd by NLDFT method from N_2 adsorption data

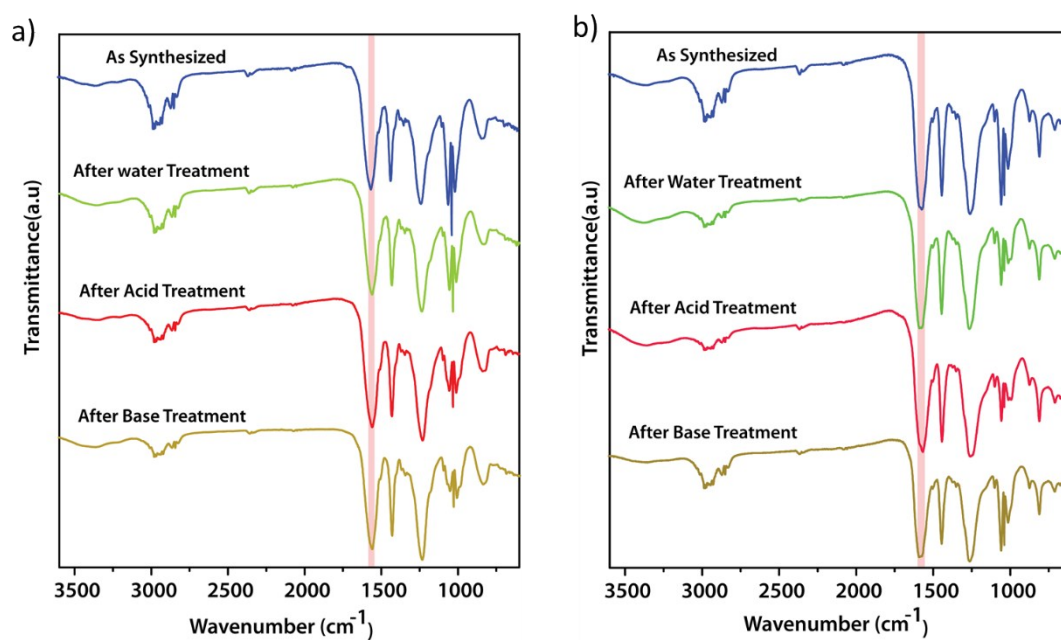


Figure S11: (a) FT-IR spectra of CAA-COF-1 after treatment with water, acid and base after 5 days, and (b) FT-IR spectra of CAA-COF-2 after treatment with water, acid and base after 5 days.

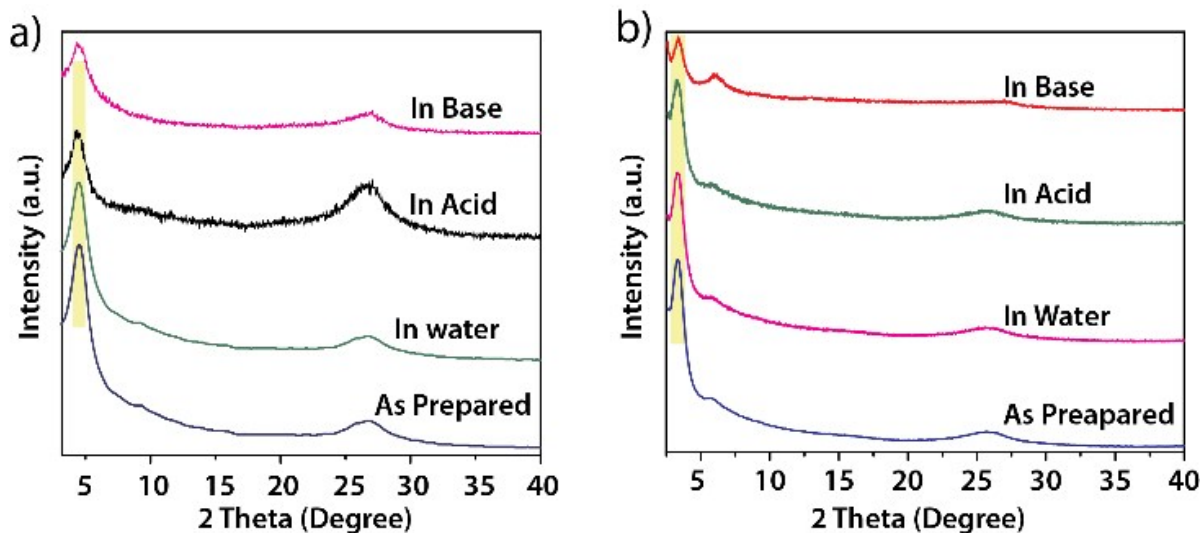


Figure S12: PXRD of CAA-COF-1 and (b) PXRD of CAA-COF-2 after treatment with water, acid and base after 5 days.

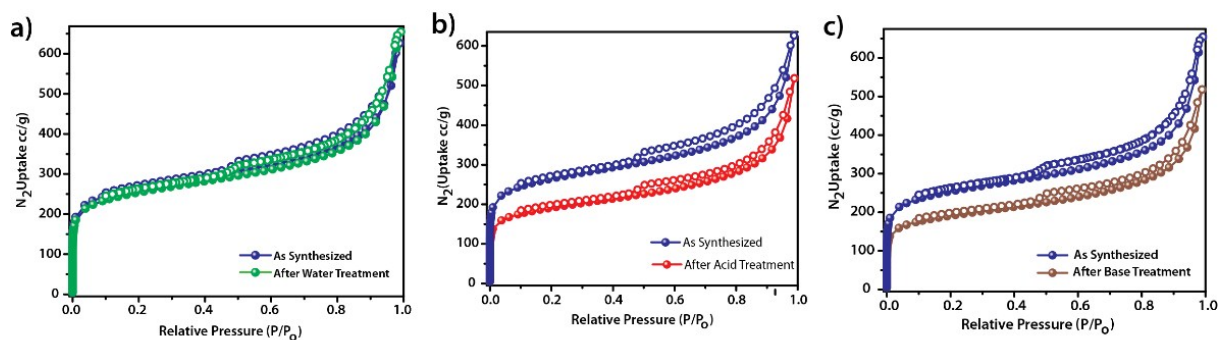


Figure S13: (a,b and c) N_2 Uptake of CAA-COF-1 after treatment with water, acid and base for 5 days.

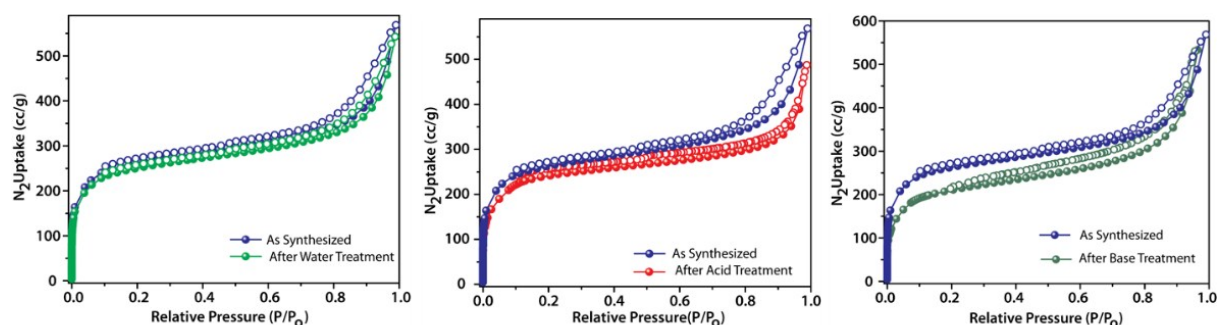


Figure S14: (a,b and c) N_2 Uptake of CAA-COF-2 after treatment with water, acid and base for 5 days.

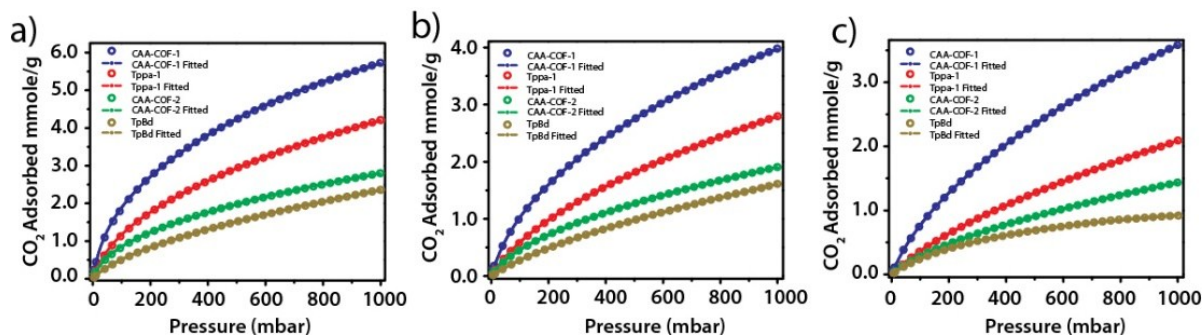


Figure S15: (a) CO₂ adsorption isotherms at 273K; (b) 298K and (c) 323K and fitted data for CAA-COF-1, TpPa-1, CAA-COF-2 and TpBd.

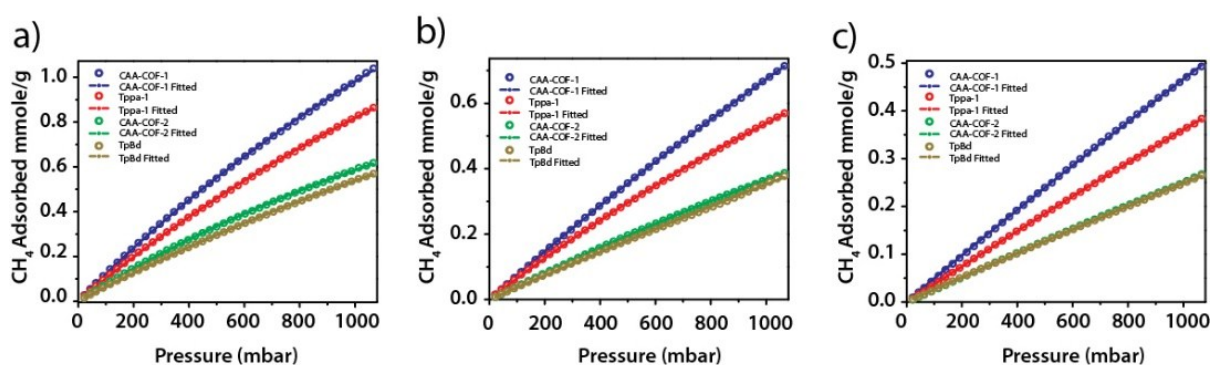


Figure S16: (a) CH₄ adsorption isotherms at 273K; (b) 293K and (c) 313K and fitted data for CAA-COF-1, TpPa-1, CAA-COF-2 and TpBd.

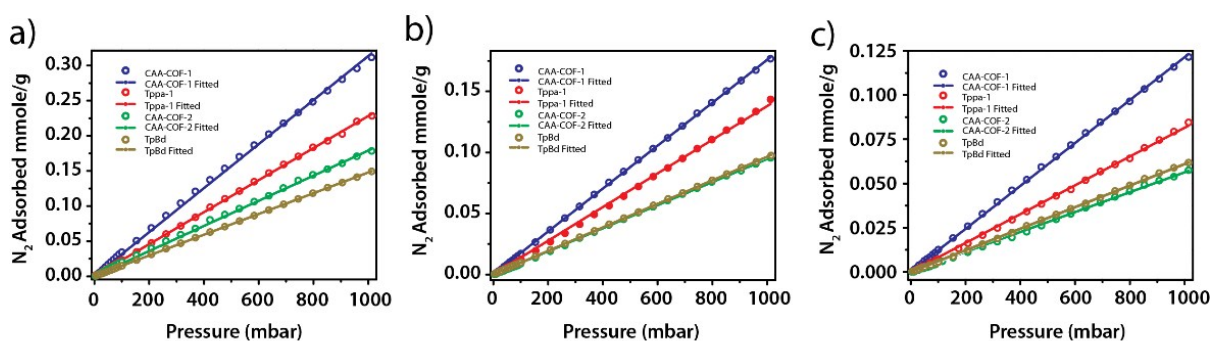


Figure S17: (a) N₂ adsorption isotherms at 273K; (b) 293K and (c) 313K and fitted data for CAA-COF-1, TpPa-1, CAA-COF-2 and TpBd.

2. Theory of Heat of adsorption and IAST calculation

2.1 Calculation of isosteric heat of adsorption (Q_{st}):

The isosteric heat of adsorption gives the prime information about the heterogeneity of the material surface as well as the interactions between gas molecules and adsorbent.

By using virial equation, calculated the isosteric heats of adsorption for (CO₂ and CH₄) adsorption isotherms measured at 273 , 298 and 323 K using the following virial equation,²

$$\ln p = \ln q + \frac{1}{T} \sum_{i=0}^m a_i q^i + \sum_{j=0}^n b_j q^j \quad \dots\dots\dots (2)$$

Where;

p: Pressure (mbar),

q: Gas uptake (mmol/g),

T: Temperature (K),

R: Universal gas constant,

a_i and *b_i*: Virial coefficients,

m and *n*: number of coefficient (m and n = 3 to 4 depending on a particular dataset).

2.2 Selectivity calculation based on the ideal adsorption solution theory (IAST):

The isosteric heat of adsorption then can be calculated from the following expression:

$$q_{ST} = -R \sum_{i=0}^m a_i q^i \quad \dots\dots\dots (3)$$

CO₂/N₂ and CO₂/CH₄ mixed gas selectivity were calculated from pure gas adsorption isotherms using the IAST (ideal adsorbed solution theory).³ For the case of CO₂/N₂, The single-component isotherms of CO₂ and N₂ were first fitted with dual site Langmuir isotherms (Equation 4).

$$q_i = \frac{q_{1,sat} k_1 p_i}{1 + k_1 p_i} + \frac{q_{2,sat} k_2 p_i}{1 + k_2 p_i} \quad \dots\dots\dots (4)$$

Where;

q_i: Gas uptake (mmol/g),

p_i : Pressure (kPa),

$q_{1,sat}$ and $q_{2,sat}$: saturation adsorption capacity (mmol/g),

k_1 and k_2 : Langmuir equilibrium constants (mbar)

The IAST theory is then applied to calculate the gas pair selectivity for a range of compositions at 101.325 kPa using the direct search minimization method.²

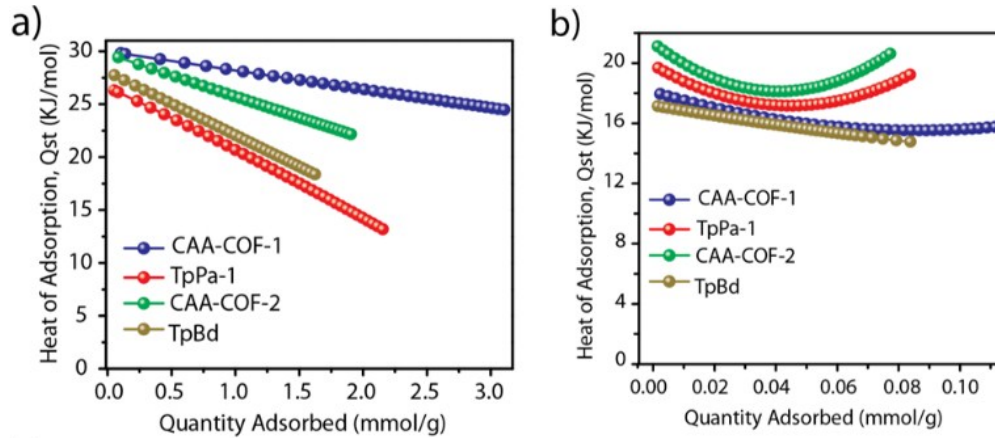


Figure S18: (a) Heat of adsorption (CO₂) for CAA-COF-1, TpPa-1, CAA-COF-2 and TpBd; (b) Heat of adsorption (CH₄) for CAA-COF-1, TpPa-1, CAA-COF-2 and TpBd .

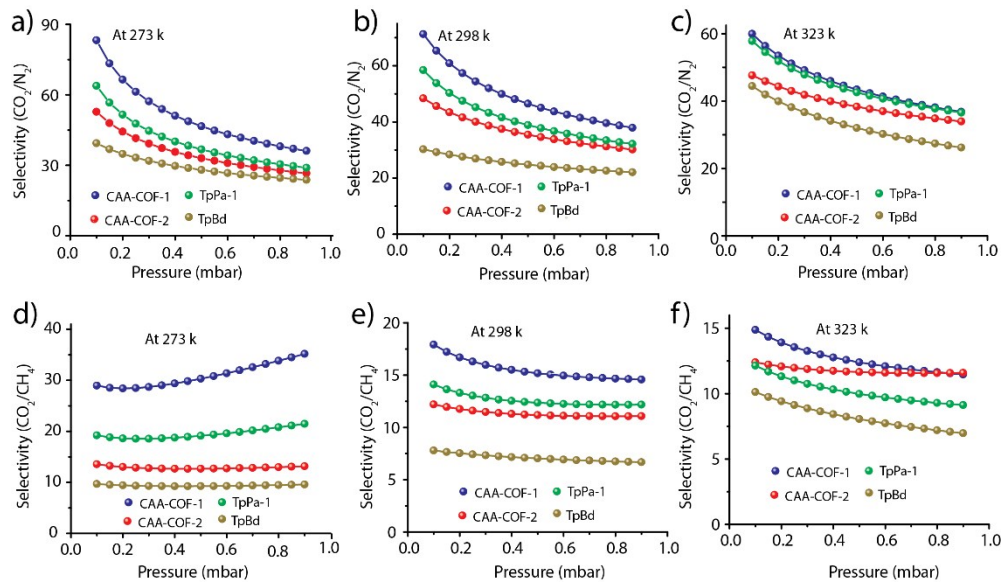


Figure S19: (a, b and c) CO₂/N₂ IAST selectivity as a function of CO₂ mole fraction at 273, 298 and 323 K for 10/90 CO₂/N₂ feed mixture for CAA-COF-1, TpPa-1, CAA-COF-2 and TpBd; (d, e and f) CO₂/CH₄ IAST selectivity as a function of CO₂ mole fraction at 273, 298 and 323 K for CAA-COF-1, TpPa-1, CAA-COF-2 and TpBd.

Table S3. Comparison of CAA-COF-1 and CAA-COF-2 with other COFs and other porous material.

Porous Material	Surface area (cc/g)	CO ₂ uptake (mmol/g)	CH ₄ uptake (mmol/g)	IAST Selectivity at 298 K		Qst (kJ mol ⁻¹)		References
				CO ₂ /N ₂	CO ₂ /CH ₄	CO ₂	CH ₄	
CU-BTC	1663	1.62	0.53	-	9	27.2	22.2	Nat. Commun. 3, (2012) 954
PECONF-1	583	1.34	0.53	51	3	29	22.2	Nat. Commun. 2, (2011) 401
PECONF-3	969	2.47	0.58	41	8	26	24.9	Nat. Commun. 2, (2011) 401
azo-COP-2	729	1.53	-	131	-	24.8	-	Nat. Commun. 4 (2013) 1357
Azo-POF-1	712	1.88	-	37	-	27.5	-	J. Mater. Chem. A, 2014, 2, 13831
BILP-2	1135	2.36	0.56	71	7	28.6	18.4	Chem. Mater. 24 (2012) 1511
[HC=C] ₅₀ -H ₂ P-COF	962	1.17	-	3	-	16.5	-	Angew. Chem. 2015, 127, 3029–3033
[EtNH ₂] ₅₀ -H ₂ P-COF	821	1.16	-	16	-	20.9	-	Angew. Chem. 2015, 127, 3029–3033
CTF-1	746	1.41	-	20	-	27.5	-	Energy Environ. Sci. 6 (2013) 3684-3692.
FCTF-1	662	3.21	-	31	-	35	-	Energy Environ. Sci. 6 (2013) 3684-3692.
CTPP	779	2.01	-	84	-	34	-	Chem. Eng. Sci.145 (2016) 21
TMCOAP	1104	2.50	-	100	15	42.2	32.7	Microporous Mesoporous Mater. 255 (2018) 76e83
CAA-COF-1	841	4.05	0.63	67.2	18.1	29.8	20.5	This work
CAA-COF-2	723	1.63	0.37	51.4	12.6	29.7	19.8	This work
Tppa-1	732	2.78	0.54	59.8	14.9	27.6	17.1	This work
TpBd	514	1.22	0.34	31.9	7.6	26.9	16.6	This work

3. Column Breakthrough

The column breakthrough experiments were carried out at 298 K.³ In this experiment, 0.5 g of CAA-COF-1 or CAA-COF-2 materials were ground well, try to make fine powder. The obtained fine powder gently packed into a column (I.D. 5.8 mm, length 150 mm), and silica wool was used for seal the ends. The packed COF materials were activated in the column with a continuous flow helium gas (5 mL/min) at 393 K for 10-12 h. After activation process, decreased the temperature to 298 K and stabilized it. After that, the feed gas was switched from helium to a gas mixture of CO₂:N₂ or CO₂:CH₄ (10: 90, v/v) at 5 mL/min. The effluent gas was monitored by a mass spectrometer (Pfeiffer Vacuum, Germany). The absolute adsorption capacity of gas *i* (q_i) is calculated from the breakthrough curve using the following equation:

$$q_i = \frac{F_i \times t_0 - V_{dead} - \int_0^{t_0} F_e dt}{m} \quad (1)$$

Where: F_i is the influent flow rate of gas *i* (mL/min),

t_0 is the total adsorption time (min),

V_{dead} is the dead volume of the system (mL),

F_e is the effluent flow rate of gas *i* (mL/min) that is calculated from the MS signal;

and m is the mass of the sample (g).

The selectivity of the breakthrough experiment is defined as:

$$\alpha = (q_1/y_1)(q_2/y_2) \quad (2)$$

Where: y_i is the molar fraction of gas *i* in the gas mixture;

The CO₂:N₂ or CO₂:CH₄ (v:v) feed compositions, 10:90 which are associated to the two boundary composition of flue gas were investigated.

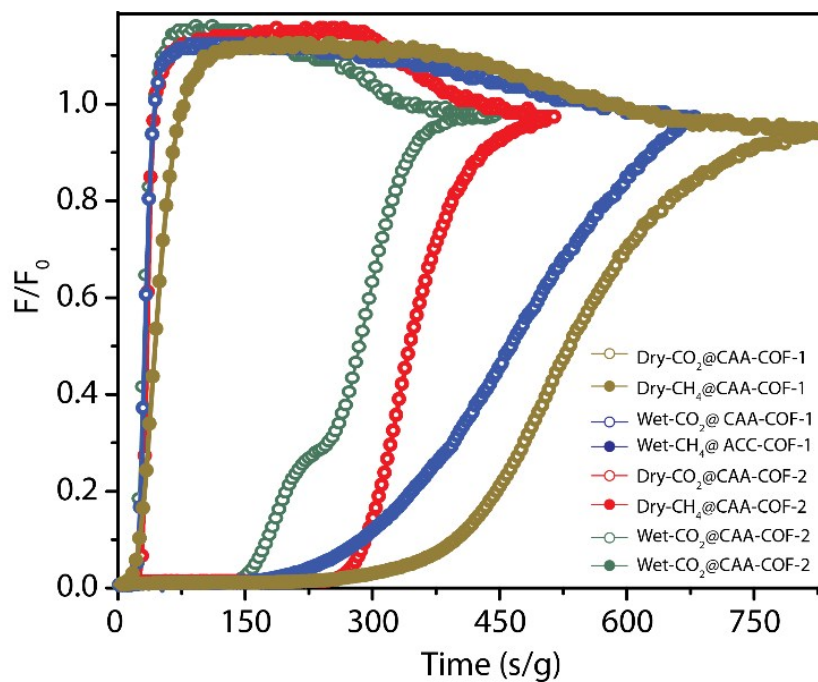


Figure S20: Column breakthrough experimental results for CAA-COF-1 and CAA-COF-2 using mixture (CO₂ and CH₄ 10:90) at dry and humid condition at 298 K.

4. References

1. J. H. Chong, M. Sauer, B. O. Patrick, M. J. MacLachlan, *Org. Lett.* **2003**, *5*, 3823.
2. (a) S. K. Das, X.B. Wang, M. M. Ostwal, Y.F. Zhao, Y. Han and Z.P. Lai; *Chem. Eng. Sci.*, **2016**, *145*, 21, (b) L. Czepirski, J. JagiełŁo, *Chem. Eng. Sci.* 1989, *44*, 797.
3. Y. Zhao, X. Liu, K. X. Yao, L. Zhao, Y. Han, *Chem. Mater.* 2012, *24*, 4725.